

## RESEARCH ARTICLE

# Application of computer vision for off-highway vehicle route detection: A case study in Mojave desert tortoise habitat

Alexander J. Robillard , Madeline Standen , Noah Giebink, Mark Spangler, Amy C. Collins , Brian Folt , Andrew Maguire , Elissa M. Olimpi  & Brett G. Dickson 

Conservation Science Partners, Inc., Truckee California, 96161, USA

## Keywords

geospatial analysis, *Gopherus agassizii*, machine learning, Mojave Desert, off-highway vehicles, recreation

## Correspondence

Brett G. Dickson, Conservation Science Partners, Inc., Truckee, CA 96161, USA. Tel: 1-530-214-8905; Fax: 1-530-214-8907. E-mail: [brett@csp-inc.org](mailto:brett@csp-inc.org)

## Funding Information

This project was funded through a cooperative agreement with the California State Office of the Bureau of Land Management (agreement number L21AC10475) and through a contract with the Department of Defense Strategic Environmental Research and Development Program (project number RC22-3182).

Editor: Dr. Temuulen Sankey

Associate Editor: Dr. Marcus Rowcliffe

Received: 18 July 2024; Revised: 18 December 2024; Accepted: 13 February 2025

doi: 10.1002/rse2.70004

## Abstract

Driving off-highway vehicles (OHVs), which contributes to habitat degradation and fragmentation, is a common recreational activity in the United States and other parts of the world, particularly in desert environments with fragile ecosystems. Although habitat degradation and mortality from the expansion of OHV networks are thought to have major impacts on desert species, comprehensive maps of OHV route networks and their changes are poorly understood. To better understand how OHV route networks have evolved in the Mojave Desert ecoregion, we developed a computer vision approach to estimate OHV route location and density across the range of the Mojave desert tortoise (*Gopherus agassizii*). We defined OHV routes as non-paved, linear features, including designated routes and washes in the presence of non-paved routes. Using contemporary ( $n = 1499$ ) and historical ( $n = 1148$ ) aerial images, we trained and validated three convolutional neural network (CNN) models. We cross-examined each model on sets of independently curated data and selected the highest performing model to generate predictions across the tortoise's range. When evaluated against a 'hybrid' test set ( $n = 1807$  images), the final hybrid model achieved an accuracy of 77%. We then applied our model to remotely sensed imagery from across the tortoise's range and generated spatial layers of OHV route density for the 1970s, 1980s, 2010s, and 2020s. We examined OHV route density within tortoise conservation areas (TCA) and recovery units (RU) within the range of the species. Results showed an increase in the OHV route density in both TCAs (8.45%) and RUs (7.85%) from 1980 to 2020. Ordinal logistic regression indicated a strong correlation ( $OR = 1.01$ ,  $P < 0.001$ ) between model outputs and ground-truthed OHV maps from the study region. Our computer vision approach and mapped results can inform conservation strategies and management aimed at mitigating the adverse impacts of OHV activity on sensitive ecosystems.

## Introduction

Habitat fragmentation poses a significant threat to biodiversity by reducing habitat quality, diminishing habitat connectivity, and imperiling species survival (USGS, 2007). A major contributor to habitat fragmentation is the legal and illegal use of off-highway vehicles (OHVs), such as dirt bikes, snowmobiles, mountain bikes, and all-terrain motor vehicles (Buckley, 2004; Monz et al., 2010). OHV

activity is known to negatively impact species across several ecosystems, like temperate woodlands (Switalski & Jones, 2012), boreal forests (He et al., 2009), wetlands (Smith, 2021), beaches (Cohen et al., 2014), and desert landscapes (Lovich & Bainbridge, 1999). The impact of OHV activities, including trail use and illegal trail creation, can negatively affect habitat quality and survivorship for many species (Lovich & Bainbridge, 1999; USFWS, 2011; USGS, 2007).

To understand the extent of OHV impacts on fragile ecosystems, comprehensive mapping of their route networks is required for effective management of threatened species, like the Mojave desert tortoise (*Gopherus agassizii*; hereafter, tortoise; Averill-Murray & Allison, 2023). OHV activities in the Mojave Desert, both legal and illegal, have long-term negative impacts on sensitive species like the tortoise (Brooks & Lair, 2005; Lovich & Bainbridge, 1999). Research has identified OHV recreation as a significant driver of tortoise population declines and reduced habitat connectivity (Averill-Murray & Allison, 2023; Boarman & Sazaki, 2006). The impact OHV activity can have on desert landscapes is believed to be extensive, with recovery estimates ranging from decades to centuries (Brattstrom & Bondello, 1983; Lovich & Bainbridge, 1999). Increased road density is linked to tortoise population decline, underscoring the importance of thorough mapping of travel networks for species recovery (Averill-Murray & Allison, 2023).

Mapping OHV networks, particularly in western landscapes like the Mojave Desert, poses significant challenges due to the lack of temporally exhaustive data and the pervasiveness of routes in non-designated areas and illegal trail networks (Averill-Murray & Allison, 2023; Sizek, 2024). For example, a prior effort mapped approximately 24 140 km of OHV routes in the western Mojave Desert using a combination of aerial imagery and direct ground truthing (US DoI, 2019). While useful, this map represents a static snapshot and cannot be used to assess changes in OHV networks over time (Sizek, 2024). Moreover, distinguishing narrow features like hiking trails and OHV routes from similar natural desert patterns (i.e., dry washes) complicates mapping efforts (He et al., 2009; Lechner et al., 2009). For these reasons, detecting a change in a comprehensive OHV route network has been described as nearly impossible (Sizek, 2024). This challenge underlines our need to innovate and understand the impacts landscape changes have on natural resources such as threatened species and the sensitive ecosystems they often inhabit.

The application of computer vision, a form of deep learning, has proven vital in leveraging large databases to answer complex conservation questions (Hoeser & Kuenzer, 2020; Weinstein, 2018) like those associated with change in OHV networks over time (Sizek, 2024). For ecology and conservation biology, combining remote sensing and computer vision helps rapidly process data and derive outcomes from challenging geospatial imagery tasks (Lamba et al., 2019; Weinstein et al., 2020). Convolutional neural networks (CNNs) process visual information through layers of interconnected nodes and excel at identifying features in data, such as detecting specific shapes across a landscape image. For example,

Weinstein (2018) and Weinstein et al. (2020) demonstrated CNNs' effectiveness in delineating tree crowns from their backgrounds across various landscapes, but noted they faced difficulties with smaller trees and trees blending into the landscape. Similarly, Van Etten (2018) encountered issues distinguishing small linear features like highways from airport runways in urban settings. Although successful, Yang et al. (2020) also noted challenges in detecting farmland borders due to similar surrounding linear features. These cases underline the potential and challenges of using CNNs to identify features that blend into their environments, such as OHV routes in desert landscapes with confounding features like dry washes (He et al., 2009; Lechner et al., 2009).

To address this complex conservation question and to inform management efforts and recovery of the tortoise, we applied computer vision cross-referenced with a preexisting static OHV route map to detect OHV routes and analyze trends in route density across the Mojave Desert ecoregion over the last five decades. More specifically, we focused our study on the range of the federally threatened tortoise to address the increasing concerns of stakeholders and experts regarding the role of OHV activities as a significant driver of the species' decline. We also aimed to better understand the potential impact of increased OHV presence on a species that is considered central to the persistence of many other species in the Mojave Desert ecoregion (Esque et al., 2021). To achieve this, we used aerial imagery from 1970 to 2022 collected from across the region and a CNN model to estimate the density of OHV routes at four unique timesteps. Our approach leveraged the strengths of a CNN in classifying images based on the presence of OHV, rather than delineating their exact boundaries, thus reducing the impact of image artifacts, and broken or obscured features common to landscape imagery while leveraging image context, enhancing our overall analysis (Hoeser & Kuenzer, 2020).

Specifically, we trained a computer vision model to recognize specific linear features as OHV routes, which include non-paved designated routes, washes in the presence of other non-paved routes, and primitive trails similar in width and geometry to traditional OHV routes. We then used our computer vision model predictions to investigate whether OHV route density has increased across the tortoise's range over the last 50 years. Finally, to identify management priority areas with high degradation risk, we calculated the percent area within extant Tortoise Conservation Areas (TCAs; defined as tortoise habitat within critical habitat, Desert Wildlife Management Areas, Areas of Critical Environmental Concern, and other protected areas, or conservation easements managed for tortoises) and Recovery Units (RUs; defined as units that are geographically identifiable and essential

to the recovery of the entire listed population; USFWS, 2011) that increased in OHV route density over the period 1980–2022.

## Methods

### Study area

We examined a ~13 million-ha study area that encompassed the range of the tortoise based on predicted habitat suitability (Nussear et al., 2009), the delineation of tortoise RUs (USFWS, 2011), and the extent of known tortoise occurrence (Allison & McLuckie, 2018) in the Mojave and Colorado Deserts of California, Nevada, Arizona, and Utah (Fig. 1). Nearly half (47.3%) of the study area is managed by the Bureau of Land Management (BLM), a multi-use mandated agency whose lands in the region include sites managed for recreation (including, specifically, OHV use), hardrock mining, livestock grazing, and renewable energy development. Other major landowners in the study area include the National Park Service (16.1%) and the Department of Defense (13.0%). This region is characterized by steep and elongated mountain ranges juxtaposed with flat, dry desert valleys dominated by creosote and bursage shrubs (Gray

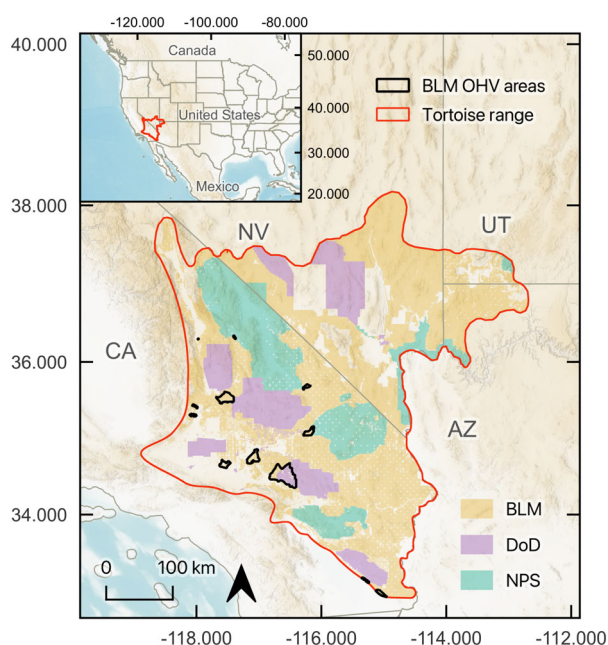


**Figure 1.** Study area (outlined in red) representing the range of the Mojave desert tortoise (*Gopherus agassizii*). Bureau of Land Management (BLM) open-use off-highway vehicle (OHV) areas in California are outlined in black. Department of Defense (DoD) and National Park Service (NPS) lands are highlighted in purple and green, respectively.

et al., 2019). For a more detailed description of the vegetation and other environmental features of the study area, see Nussear et al. (2009).

### Aerial imagery

To model OHV routes across the range of the tortoise, we leveraged publicly available and privately managed image sources (Table 1). Collated historical aerial imagery for the 1970s and 1980s was procured from the BLM National Operations Center (NOC) and Historical Aerials (Nationwide Environmental Title Research, LLC; NETR). We obtained historical imagery from NETR and NOC at multiple spatial resolutions (Table 1). We also acquired USGS digital orthophoto quadrangle (1-m resolution) scenes for the years 1990–2003 (USGS, 2018). However, we were unable to use these data for modeling OHV routes due to inconsistent quality (e.g., discolored images, various resolutions provided) and spatial coverage. Although the historical imagery we used also had inconsistencies, these were less frequent and did not prevent effective preprocessing and image cleaning. For the years 2003–2022, we used geospatial tiles from the U.S. Department of Agriculture National Agriculture Imagery Program (NAIP; 1-m resolution) acquired through Google Earth Engine (Gorelick et al., 2017), which offered the broadest contemporary spatial coverage, though coverage varied by state and year as per NAIP's data collection protocol (USDA, 2022). We also observed some image artifacts in the contemporary imagery predominantly around the 2010 time period, but similar to the historical imagery, over a much smaller extent than the 1990's data. All scenes were projected to a common coordinate reference system (EPSG: 3857; a web-Mercator projection)

**Table 1.** Outline of the unaltered quality, source, and temporal range of aerial imagery used for off-highway vehicle route density detection model development.

Timestep	Temporal coverage	Native resolution (meters)	Source
1970s	1970–1979	0.4–1.0	NETR, NOC
1980s	1980–1989	0.7–0.8	NETR
2010s	2010–2012	0.6–1.0	NAIP
2020s	2019–2022	0.6–1.0	NAIP

The table includes the representative timesteps used in modeling, the years included in each timestep, the range of spatial resolution, and the source of corresponding aerial imagery datasets. Geospatial data were sourced from the U.S. Department of Agriculture National Agriculture Imagery Program (NAIP), Bureau of Land Management National Operations Center (NOC), and Nationwide Environmental Title Research, LLC (NETR).

and resampled to a 1-m resolution grid for consistency in subsequent processing. Our curated collection of historical (1970–1989) and contemporary imagery (2010–2022) was then organized into four individual timesteps, with each step representing a composite mosaic of images from different years from a given temporal snapshot (Table 1).

### Image preprocessing

Prior to modeling, we implemented image quality control measures to address the occurrence of image artifacts on the selected landscape imagery. Although usable, some tiles of the 2010 timestep required intensive removal of artifacts and other image quality issues introduced by multiscene mosaicking. Artifacts and other image quality issues were also present in the 1970s and 1980s data but to a much lesser extent and appeared largely due to side effects of digitization. Many of these notable artifacts manifested as linear features on mosaicked scenes, which propagated erroneous detection of OHV features on the landscape through image classification modeling. To correct this, we utilized a multistep preprocessing approach to identify, mask, and smooth over these artifacts. Specifically, we used a modified Sobel filter in R (R Core Team, 2018), which detects changes in pixel intensity across a two-dimensional gradient to aid identification of edges in imagery (Vincent & Folorunso, 2009). Application of our Sobel filter resulted in the generation of geospatial imagery ready for ingestion into our computer vision algorithm (see Appendix S0 for more details about our Sobel filter and other preprocessing steps).

### Computer vision data curation, annotation, and model training

To identify OHV route density, we developed our own set of OHV image classification models using a Nvidia

Tesla (V100; 32GB VRAM) GPU and the Fast.ai library (Howard & Gugger, 2020) in PyTorch (Paszke et al., 2019) deployed on Microsoft Azure. We utilized an image classification model instead of a segmentation model as it might generalize better to detect truncated, broken, and obscured features, or otherwise visually variable features common to earth observation image sets (Hoeser & Kuenzer, 2020). Our models were constructed using a Resnet-101 architecture (He et al., 2016) pre-trained on the ImageNet dataset (Deng et al., 2009). We selected a type of image classification model due to its cost-efficiency and effectiveness in generalizing across highly variable landscapes (Hoeser & Kuenzer, 2020). This enabled us to classify OHV route density within a given 150 m x 150 m (0.0225 km<sup>2</sup>) area, hereafter referred to as a raster cell (Fig. 2).

We considered the quality of the contemporary image data to be acceptable, but variable in space and time. For example, the majority of the contemporary imagery was full color and generally mosaicked without visible seams between images. This is in contrast to the historical data, which had minor image tearing, processing artifacts, and variable lighting and coloration (i.e., both black and white, and color imagery) even after the application of our Sobel filter. Although usable, the historical image quality was lower than that of the contemporary image data. When presented with lower quality imagery, past research has suggested the application of a ‘hybrid’ approach of supplementing lower-quality imagery with additional higher quality images that can boost the performance of computer vision models (Lendemer et al., 2020; Robillard et al., 2023). To account for differences in image type and quality, we developed three different convolutional neural network (CNN) computer vision models: one model was trained only on image data from 2010 to 2022 (contemporary model), one model was trained only on image data from 1970 to 1989

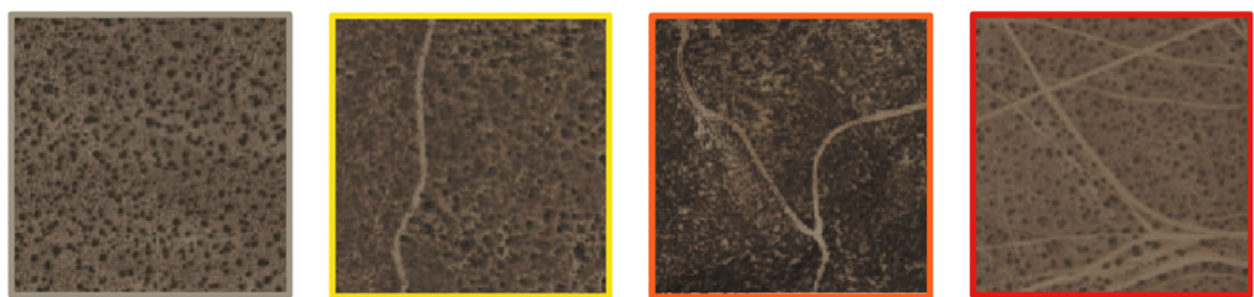


**Figure 2.** Example images from computer vision model classifications that were used to measure off-highway vehicle (OHV) route density and quantify changes in density through space and time in the Mojave Desert ecoregion. We trained models to classify images into one of four categories: none (gray panel; 0 m OHV), low (yellow panel; ≤150 m OHV), medium (orange panel; 151–450 m OHV), and high (red panel; 451–22 500 m OHV). Each category represents an estimate of the relative density of OHV routes within a given output raster cell.

(historical model), and one used both datasets to train a ‘hybrid’ model (see Fig. S1 in Appendix S1 for more details on our computer vision pipeline).

To develop our training dataset, we resampled aerial imagery to a uniform 1-m resolution. Contemporary image tiles were derived specifically from across BLM-designated ‘open-use’ OHV areas in southern California, which offered abundant OHV route imagery, using the ‘terra’ package (Hijmans et al., 2022) in the statistical program R (R Core Team, 2018). Image tiles were randomly sampled without overlap, and each tile was split into smaller 0.0225 km<sup>2</sup> images ( $n = 11\,098$ ). These images were then visually categorized by three reviewers into one of four classes (Fig. 2) based on the approximate amount (i.e., linear distance) of OHV routes in a given image. Images were classified into ‘none’ (no OHV routes detected), ‘low’ (1–150 m of OHV route present), ‘medium’ (151–450 m of OHV route present), and ‘high’ (451–22 500 m of OHV route present). Given that each image was a square, uniformly 0.0225 km<sup>2</sup>, this made the classification by OHV trail length approximation relative to the known cell size (see Appendix S1 for more details on the data annotation process).

An additional consideration was the visual similarities between linear features such as dry-riverine habitats (certain-sized desert washes) and OHV routes and roads. To account for the influence washes might have on OHV route density estimates, reviewers were instructed to only label washes as potential OHV routes if they were directly associated with an OHV route in the same image; this standard was applied to both historical and contemporary datasets. Building on past research showing that washes are often used for OHV recreation (Custer et al., 2017), we refined our model to detect only washes similar in size and shape to OHV routes. From an aerial perspective, OHV routes appeared uniformly straight and thick, contrasting with the winding, variable-width washes. We excluded paved roads and urban streets from the OHV route density categories and discarded images with processing artifacts during training. The final combined hybrid dataset of reviewed images ( $n = 2647$ ) was composed of a balance of contemporary ( $n = 1499$ ) and historical ( $n = 1148$ ) images. In each instance, 20% of the image data was withheld from training for validation, while the remaining 80% of the data was utilized for model development (Table 2).

## Model testing, validation, and deployment

Given the varying image quality of our datasets, we developed three different test sets to benchmark the performance of our three models. We randomly selected images from areas not used in either training effort, from along

**Table 2.** Computer vision training and testing results for the three off-highway vehicle route density models.

Model	Training epochs	Training images	Validation images	Validation accuracy
Contemporary	60	1200	299	79.9
Historical	134	919	229	75.8
Hybrid	73	2118	529	78.3

‘Training epochs’ represents the length of time the models were trained for. ‘Training images’ is the total count of images used to train a model. ‘Validation images’ is the number of images held apart from training to iteratively measure model accuracy. ‘Validation accuracy’ is the percentage of correctly identified images by the final iteration of the model.

southern California and along the southern Nevada–California border for each of these datasets. Using novel data to test our models is a standard practice in deep learning to ensure generalization and to avoid overfitting models (Goodfellow et al., 2016). We scored images with three reviewers and included results in the final test effort. Test sets were developed for both contemporary ( $n = 956$  images) and historical ( $n = 851$  images) datasets (Table 3). Finally, we generated a hybrid dataset with an equal random selection of data from both the contemporary and historical test sets ( $n = 1807$  images) (Table 3). For deployment, we selected our best model, the hybrid (Table 3), based on its F1 score. The F1 score demonstrates a balance between the model’s precision (correctness) and recall (comprehensiveness) (Goodfellow et al., 2016). Deploying this model, we estimated the OHV route density across the study area using all available data for each of the four timesteps. Based on these results, we produced a spatial data layer for each timestep with a resolution of 0.0225 km<sup>2</sup>. We then processed our OHV route density layers using a two-part cleaning and masking protocol (see Appendix S2 for more details).

## Model evaluation

To further verify that our computer vision algorithm estimated OHV route density with high accuracy, we used a spatial dataset of approximately 24 140 km of known, ground-truthed OHV routes completed in 2013 as part of the BLM’s West Mojave Route Network Project (WMRNP; US DOI, 2019). Routes were inventoried during 2012–2013 both in the field with handheld GPS equipment and by review of high-quality aerial imagery from 2009 by GIS personnel (for further details see US DOI, 2019, Chapter 1, Section 1.1.4). We generated a spatial data layer representing the density (total length per cell) of these known OHV routes at the same resolution (0.0225 km<sup>2</sup>) as the OHV computer vision algorithm

**Table 3.** Summary of results for off-highway vehicle route density model benchmarking across the three test sets.

Model	Historical data ( <i>n</i> = 851)				Contemporary data ( <i>n</i> = 956)				Hybrid data ( <i>n</i> = 1807)			
	Accuracy	Recall	Precision	F1	Accuracy	Recall	Precision	F1	Accuracy	Recall	Precision	F1
Historical (trained on 1970–1989 imagery)	0.70	0.70	0.82	0.69	0.59	0.59	0.40	0.48	0.64	0.61	0.57	0.59
Contemporary (trained on 2010–2022 imagery)	0.48	0.48	0.24	0.32	0.73	0.73	0.69	0.71	0.61	0.61	0.57	0.55
Hybrid (trained on combined imagery)	0.78	0.78	0.76	0.77	0.77	0.77	0.75	0.76	0.77	0.77	0.75	0.76

Metrics include: 'accuracy' (the percentage of correctly identified images to the total number of images tested on), 'recall' (the ratio of 'true positives' to the sum of true positives and false negatives), 'precision' (the ratio of true positives to the sum of true positives and false positives), and 'F1' (the harmonic mean of recall and precision). Sample size (*n*) is representative of the number of images in each dataset.

outputs. We then used an ordinal logistic regression model (MASS v7.3–60.2; Ripley & Venables, 2002) to test the relationship between the density of these known OHV routes and the probability of a raster cell belonging to a given predicted OHV route density category in the processed 2010 decadal output. As the exact spatial extent of the area inventoried for the WMRNP was not available to us, we limited this analysis to raster cells for which there was both an OHV route density estimate and a known route density value greater than 0 (*n* = 112 369). The area included in this validation analysis was 2528.30 km<sup>2</sup>, or approximately 1.01% of the entire area of the tortoise's range.

## Trend analysis

To assess the utility of the data products generated from our computer vision model to tortoise conservation and natural resource management in the Mojave Desert, we calculated the total area in every TCA and RU (USFWS, 2011) in each of the OHV route density classes (low, medium, and high) using the 1980 and 2020 timesteps to maximize our temporal view. As a measure of quality control, we did not use the 1970 timestep given the relative incompleteness of its spatial coverage compared to the other timesteps (See Table 3). Additionally, we calculated the total area and percent cover in every TCA and RU exhibiting an increase in OHV route density class over the 1980–2020 timesteps.

To evaluate range-wide temporal change in OHV route density, we estimated the minimum and median total length of OHV routes within the Mojave Desert ecosystem at each timestep. We estimated the minimum and median total length of OHV routes to ensure our totals were conservative and did not provide a maximum estimate due to the uncertainty regarding the maximum possible OHV route density that could be represented by the 'high' category. To test the hypothesis that OHV route

density has increased across the tortoise range over the last 50 years, we used binomial logistic regression in the 'lme4' R package (v1.1–35.3; Bates et al., 2015) to model the effect of year on the likelihood that a given raster cell contained OHV routes. To test the effect of year, we associated each raster cell value with the year at the end of the range of years included in a given decadal timestep (i.e., for the 1970s decade, we associated the 1970s raster cell values with the year 1979). We accounted for non-independence stemming from repeated sampling in space through time using a unique value for each raster cell as a random effect and accounted for spatial and temporal variation in image quality using a tile-by-year random interaction effect. We then mapped the magnitude of the increase in OHV route density from 1980 to 2020 timesteps (see Appendix S3 for details on methods related to trend visualization and Appendix S4 for details on regression modeling).

## Results

### Computer vision model testing and deployment

Test efforts suggested that our models were benchmarked with a broad range of results, with accuracies ranging from 40% to 78% (Table 3). Most notably, the hybrid model reached an accuracy of 77% with an F1 of 0.76 against a hybrid test set (Fig. 3). For the range of the tortoise, we classified a total of 39 707 905 unique raster cells across all four timesteps (Fig. 4), amounting to a total area analyzed of 893 428 km<sup>2</sup> (Table 4).

### Evaluation

The ordinal logistic regression model of known OHV route density and computer vision model predictions indicated a significant positive relationship (OR = 1.01,

		Hybrid model vs Hybrid validation set		
		High	Medium	Low
Actual Class	High	53	22	2
	Medium	50	148	70
Low	3	84	303	75
None	4	13	33	888

**Figure 3.** Confusion matrix of hybrid model test classification accuracy. The model yielded an accuracy of 0.77 ( $n = 1807$  images) and an F1 of 0.76. The Y-axis represents the 'Actual class' an image belongs to, while the X-axis is the model's 'Predicted class'. The number within each box represents counts of predicted vs. actual images. Squares with correct (diagonal) and incorrect (off-diagonal) images are colored based on the relative density of their classification (darker blue means more in the category).

$P < 0.001$ ) between known route density and predicted OHV route density category. For each 100-meter increase in known OHV route length within a given raster cell ( $\sim 0.0225 \text{ km}^2$ ), there were 89.4% greater odds of that raster cell having a higher associated OHV route density category (87–92%, 95% CI,  $P < 0.001$ ). Of the categories containing OHV route features, low had the greatest probability from 0 to 214 m, medium from 215 to 392 m, and high had the greatest at  $>392$  m. Shifts in probabilities of OHV route density categories low, medium, and high generally reflected the amount of OHV route denoted by each category (none = 0 m, low = 1–150 m, medium = 151–450 m, and high  $\geq 451$  m) (Fig. 5).

### Trend analysis

For raster cells with OHV route density estimates at each timestep (66% of the total range area), we observed an overall increase between the 1980s and 2020 timesteps in the total length (Fig. 6) and density of OHV routes (Fig. 7). Our overall OHV route length increased by 80.3% for the minimum estimate and 108.9% for the median estimate. Regression modeling demonstrated an increase in OHV route density (OR = 1.11,  $P < 0.001$ ) in the Mojave Desert ecosystem over the time period between 1970 and 2022. The odds of a given raster cell containing one or more OHV routes were predicted to be

5.8 times higher (5.4–6.3, 95% CI) for each year that passed between 1979 and 2022. Estimates of OHV route density in each of the TCAs and RUs suggested an overall increase in OHV activity in these areas from 1980 to 2020 (Table 5). On average, RUs exhibited an increase in OHV route density across 7.85% of their area ( $SD = 1.32\%$ , range = 6.05–9.45%) and TCAs exhibited an increase in OHV route density across 8.45% of their area ( $SD = 1.61\%$ , range = 6.74–12.73%). See Appendix S5 for more details on trend analysis results.

### Discussion

Our results demonstrate that a computer vision model was capable of detecting OHV routes and estimating route density with relatively high accuracy for a period spanning more than five decades. To our knowledge, this is the first effort of its kind for a dynamic desert environment. Our accuracy estimates are consistent with those yielded by machine learning approaches used to detect linear features across other complex landscapes, including agricultural (Yang et al., 2020), urban (Najjar et al., 2017), and industrial areas (Van Etten, 2018). Importantly, a comparison of our model output with known OHV route locations substantiates our finding, which suggests that the prevalence of OHV routes has increased significantly over the region and time period of analysis. Specifically, our results suggest OHV activity increased across TCAs and RUs between 1980 and 2020 (see Appendix S6 for more details). Although this trend has previously been identified within a more limited temporal scale (Brooks & Lair, 2005), ours is the first effort to quantify and map such a trend with broad spatial coverage and multidecadal resolution.

Evaluation of our hybrid model via a confusion matrix demonstrated an overall accuracy of 77%. As the classification of cells in the 'no OHV route' class scored an accuracy of 94.7%, the majority of the model misclassifications stemmed from cells with one or more OHV routes. When linear features are present, misclassification can occur in the form of either overestimation or underestimation (Goodfellow et al., 2016). Overestimation occurs when the model predicts more linear features than actually exist, leading to a higher false positive rate (approximately 7.66%). Conversely, underestimation happens when the model predicts fewer features than present, resulting in a higher false negative rate (approximately 22.97%). Though such detection error exists in our model outputs (<23% of cells), this includes both overestimation and underestimation, and as such still permits us to conservatively measure overall patterns and changes in OHV route features and density in space and time.

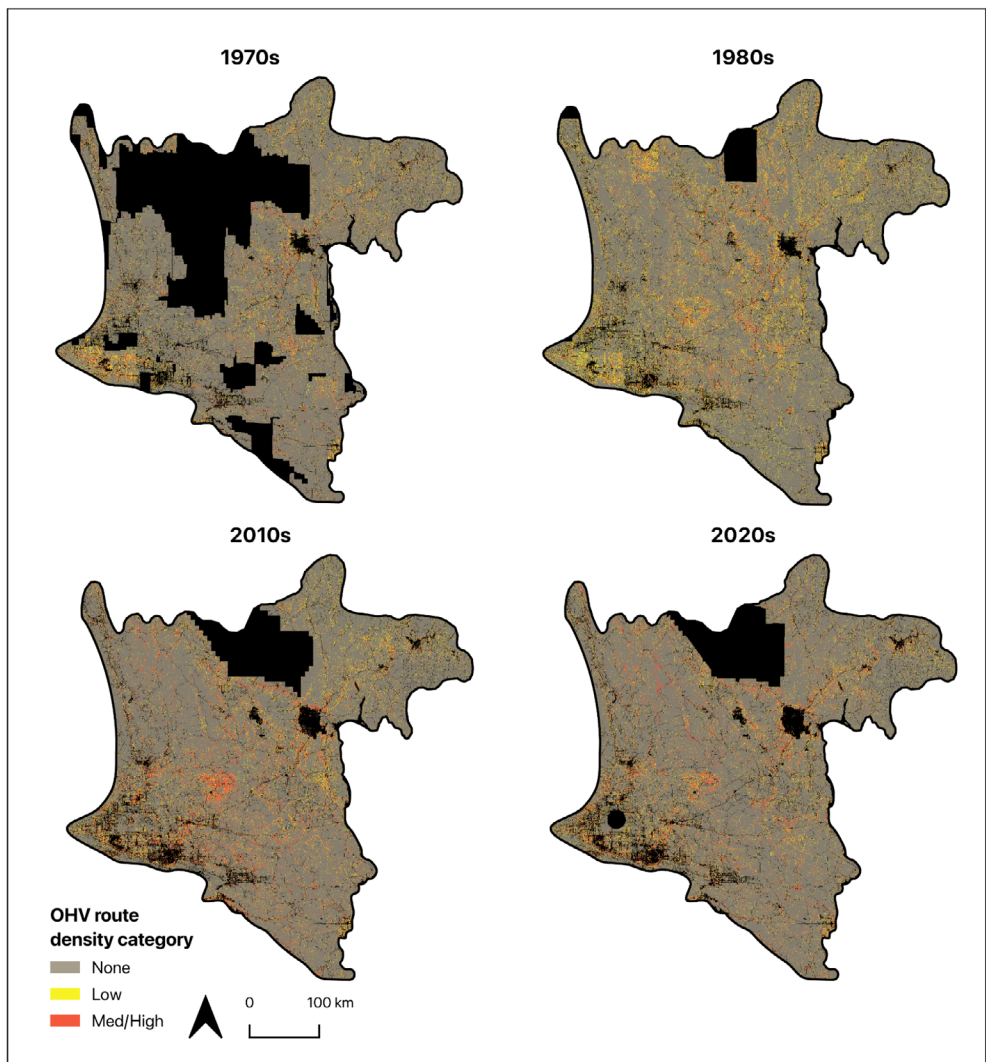


**Figure 4.** Off-highway vehicle (OHV) route density maps encompassing the range of the tortoise in the Mojave Desert ecoregion generated for four decadal timesteps (1970s, 1980s, 2010s, and 2020s) using aerial imagery and a computer vision model. Output categories from the computer vision model are: 'none' = no OHV routes; 'low' = up to 150 m of OHV route; 'medium' = 151–450 m of OHV route present; and 'high' = 451–22,500 m of OHV route present. Categories medium and high were combined for visualization purposes. Areas in black reflect the presence of open water or developed areas (Dewitz, 2023; Sohl et al., 2016), designated paved roads (US Census Bureau, 2022), or where source imagery data were unavailable.

Our implementation of an image classification approach, rather than a segmentation model (Hoeser & Kuenzer, 2020), allowed us to focus on identifying and locating OHV routes without the need for precise delineation and differentiation of every feature in our training data, which there are innumerable on a complex landscape. Using image classification also greatly reduced the time and cost spent on data annotation and computation (Csurka et al., 2022) while allowing us to maintain a similar expectation of accuracy to a segmentation model (Giorgiani do Nascimento & Viana, 2020). In addition,

image classification models are particularly effective in generalizing across the highly variable landscapes common to remotely sensed data, including different orientations, densities, and partial obscurity of features (Hoeser & Kuenzer, 2020). Image classification models effectively generalize across variable landscapes in remotely sensed data, handling different orientations, densities, and partial obscurity of features (Hoeser & Kuenzer, 2020).

Visual inspection of our model results indicates that high-density OHV areas, such as those near urban centers like Nellis Dunes OHV Recreation Area, were occasionally

**Table 4.** For each timestep, the number of raster cells classified in computer vision output layers, the total area, and the percent of area analyzed in our classification of off-highway vehicle route density across the range of the tortoise in the Mojave Desert ecoregion in southern California.

Timestep	Number of raster cells classified	Total area (km <sup>2</sup> )	Percent of range area (%)
1970s	8 090 344	182 032.74	72.93
1980s	10 862 633	244 409.24	97.93
2010s	10 396 239	233 915.38	93.72
2020s	10 358 689	233 070.50	93.38
<b>Total</b>	<b>39 707 905</b>	<b>893 427.86</b>	

misclassified, making areas of intense use appear similar to open desert landscapes, particularly in BLM open-use areas and dry lake beds. Notably, our computer vision pipeline used a single geospatially referenced image of a 0.0225 km<sup>2</sup> area and classified the density of OHV routes in that raster cell. Future improvements to our computer vision model could incorporate a multiscale context approach (e.g. Xie et al., 2018), which would provide additional information (e.g., consideration of adjacent, intact segments of routes) to better identify more challenging areas such as those extreme cases of intense usage or areas with lower quality imagery (e.g., historical imagery).

Despite observing artifact issues with source imagery in our image preprocessing steps, these issues were negligible after preprocessing and led to only minor discrepancies in our estimation of OHV route density. Nevertheless, developing a model to detect OHV routes from remotely sensed imagery presents a significant challenge due to uncertainties around defining an OHV route (Westcott & Andrew, 2015). Documented use of washes for OHV recreation (Custer et al., 2017) led us to include images of washes, but limited inclusion only to instances that clearly included recognizable OHV routes and washes in them. Visual inspection of our results suggests we successfully excluded the majority of smaller washes (i.e., lower order hydrologic features) and many large washes (higher order). However, our model did detect some medium-sized (mid-order) washes, which appeared similar to OHV routes in our source imagery. Without extensive ground truthing of these mid-order washes across the region, we cannot definitively state their use as OHV routes, but we acknowledge their potential for such use.

By leveraging spatial insights from our findings, managers can use our map-based products to prioritize enforcement and restoration efforts in regions experiencing the greatest ecological disruption. Although our model results are not intended to pinpoint the exact locations of every route, we believe our map-based products can be a useful aid in effectively mitigating OHV-related

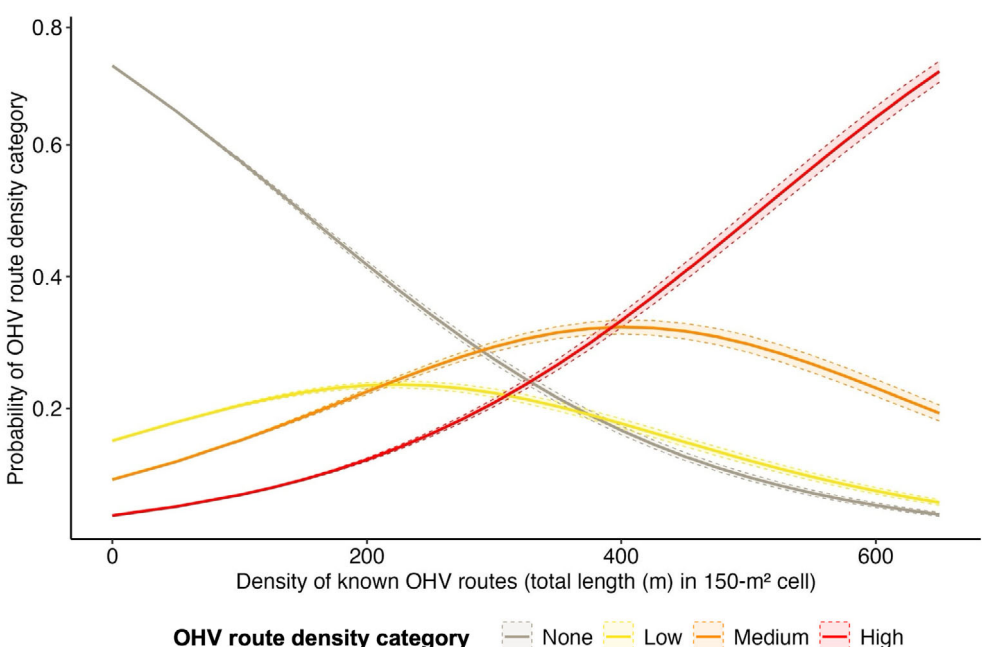


**Figure 5.** Predicted probability of a given raster cell belonging to each off-highway vehicle (OHV) route density category at different densities of known OHV routes based on an ordinal logistic regression model of known OHV routes (U.S. Department of the Interior, 2019) and our computer vision model predictions. A 95% confidence interval is denoted by dashed lines and shading.

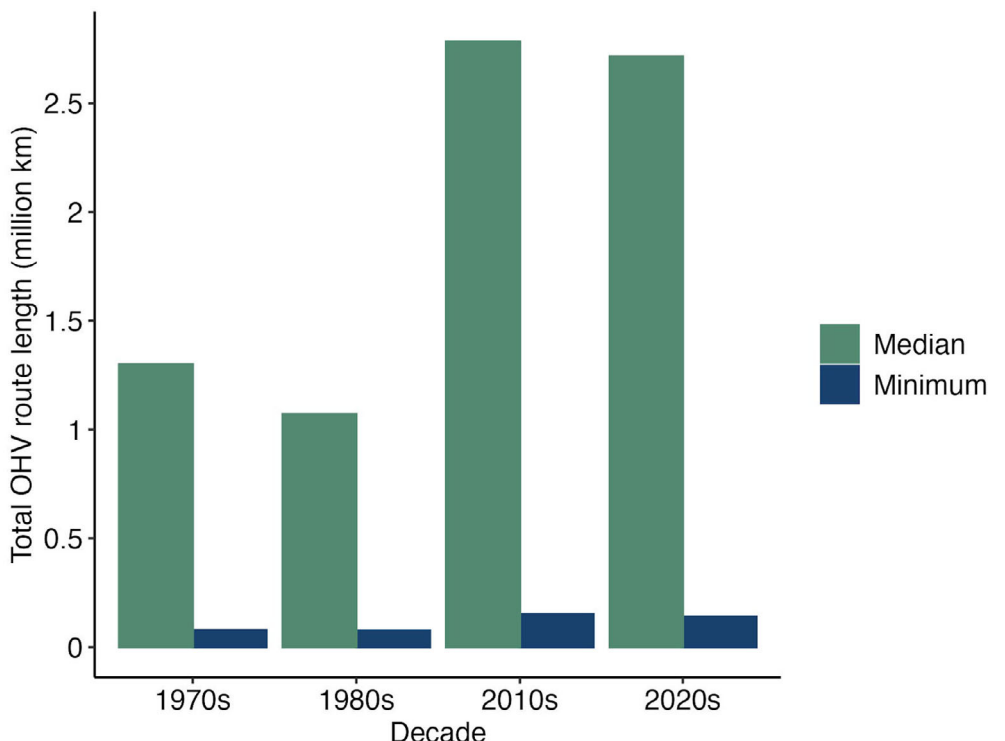


**Figure 6.** Estimates of total median (green) and minimum (blue) OHV route length across the range of the tortoise in the Mojave Desert ecoregion across four timesteps. The minimum estimate was calculated using the OHV route density classification: 'low' = 1 m of OHV route per raster cell, class 'medium' = 151 m, and class 'high' = 451 m. The median estimate was calculated using the OHV route density classification: 'low' = 75 m of OHV route per raster cell, 'medium' = 300 m, and 'high' = 11,475 m. Estimates only included cells for which there was a model-based estimate of OHV route density for each timestep. For reference, we also calculated the maximum theoretical amount of OHV within a cell as 22,500 m.

impacts. The insights gained from our study provide a foundation for expanding the application of these methods to other systems where OHV routes and similar linear features pose threats to biodiversity. Woodland, montane, beach, and wetland ecosystems, which also face significant ecological pressures from recreational trail networks, could benefit from similar detection approaches (Cohen et al., 2014; He et al., 2009; Smith, 2021; Switalski & Jones, 2012). Similar methods as those demonstrated here could be applied to other areas where OHV route detection would benefit ecosystem management, such as areas impacted by intense poaching, which are facilitated by OHV route networks (Switalski & Jones, 2012). Beyond OHV routes, the techniques demonstrated here can be adapted to detect other linear features, such as pipelines, fences, and powerlines, which fragment habitats and alter wildlife movement (Jakes et al., 2018; Richardson et al., 2017).

Further research that integrates computer vision with collated archival and contemporary remotely sensed data will be pivotal in addressing complex conservation questions. Future research should concentrate on refining

these models to enhance their accuracy and performance in challenging environments. This includes incorporating multiscale contextual analyses to improve feature detection and utilizing modern high-resolution imagery to broaden their applicability. By advancing the capabilities and extending the scope of these approaches, we can deepen our understanding of the ecological impacts of human infrastructure and develop more effective tools for conservation and land management across varied landscapes.

## Acknowledgments

This project was funded through a cooperative agreement with the California State Office of the Bureau of Land Management (agreement number L21AC10475) and through a contract with the Department of Defense Strategic Environmental Research and Development Program (project number RC22-3182). We are thankful to J. Brislain and K. Harris for annotating aerial imagery. Additionally, we thank A. Fesnock with the California State Office of the Bureau of Land Management for support

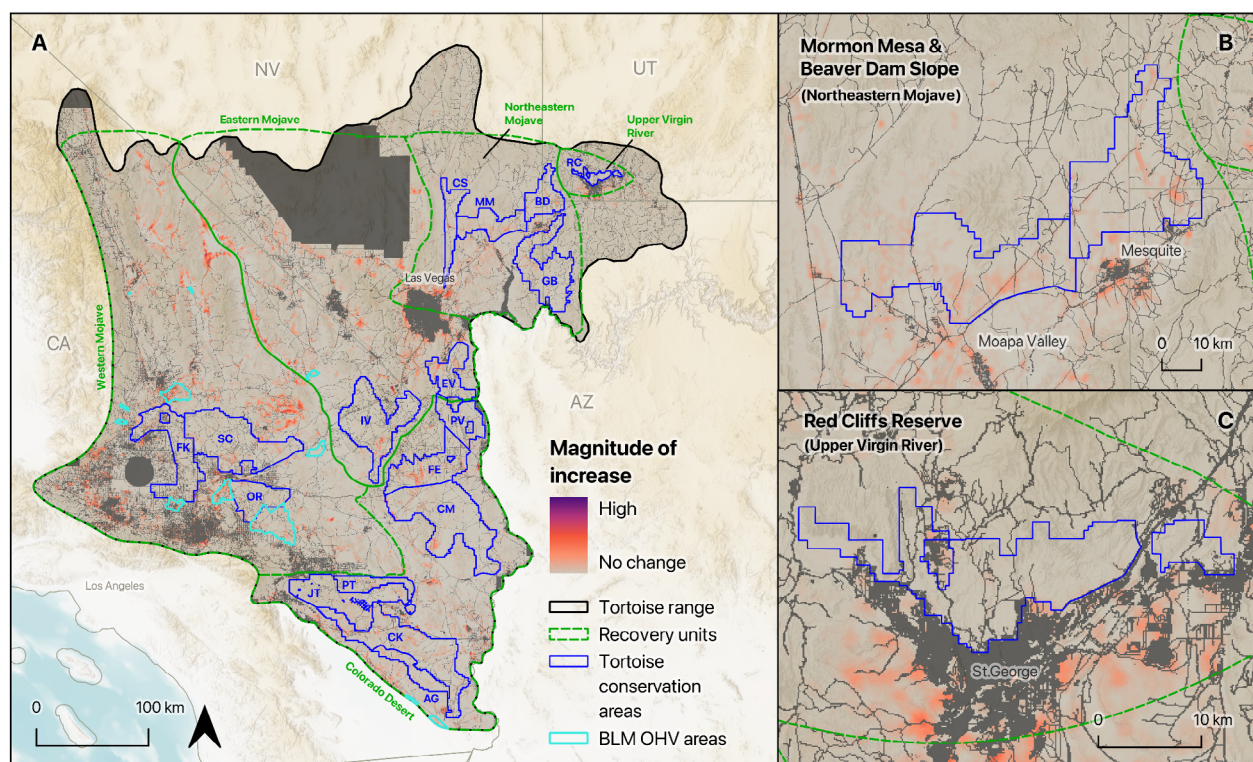


**Figure 7.** (A) Magnitude of off-highway vehicle (OHV) route density increase between the 1980s and the 2020s timesteps across the approximate range of the Mojave desert tortoise (*Gopherus agassizii*). ‘Tortoise conservation areas’ (blue border) and their corresponding ‘recovery units’ (green dashed border) are highlighted for management and conservation prioritization (USFWS, 2011), as well as Bureau of Land Management (BLM) open-use OHV areas in California. (B) Mormon Mesa and Beaver Dam Slope Tortoise Conservation Areas in the Northeastern Mojave Recovery Unit and (C) Red Cliffs Reserve Tortoise Conservation Area in the Upper Virgin River Recovery Unit. Dark gray areas reflect the presence of impervious surfaces, water, or roads that were masked out during layer processing, or where source imagery data were unavailable. Tortoise conservation areas are labeled as follows: AG = Chocolate Mountain Aerial Gunnery Range; BD = Beaver Dam Slope; CK = Chuckwalla; CM = Chemehuevi; CS = Coyote Springs; EV = Eldorado Valley; FE = Fenner; FK = Fremont-Kramer; GB = Gold Butte-Pakoon; IV = Ivanpah; JT = Joshua Tree National Park; MM = Mormon Mesa; OR = Ord-Rodman; PT = Pinto Mountains; PV = Piute Valley; RC = Red Cliffs Reserve; SC = Superior-Cronese.

and the Bureau of Land Management National Operations Center for digitizing and sharing their aerial imagery. Lastly, we appreciate the comments of S. Sesnie, J. Suraci, and three anonymous reviewers, which greatly improved the final manuscript.

## Author Contributions

Alexander Robillard: Developed and executed study design, trained computer vision models, a primary contributor to manuscript writing, manuscript review, data acquisition, assisted with cloud pipeline development, interpretation of data, and statistical analysis. Madeline Standen: Processed computer vision inference output, designed post-processing protocol, and assisted with statistical analysis, manuscript writing, and review. Noah Giebink: Developed and executed cloud deployment of

computer vision models, assisted in study design, data acquisition, training and validation data annotation, and manuscript review. Mark Spangler: Assisted with study concept and design, data acquisition, training, and validation data annotation, manuscript writing, and review. Amy Collins: Assisted with study design, geospatial analysis, data acquisition, and manuscript writing, and manuscript review. Brian Folt: Assisted with study design, data interpretation, statistical analysis, manuscript writing, and manuscript review. Andrew Maguire: Developed and deployed the data pre-processing pipeline, contributed to manuscript writing and manuscript review, and offered conceptual guidance and geospatial data interpretation. Elissa Olimpi: Assisted with data interpretation, manuscript writing, and review. Brett Dickson: Acquired funding for the project, provided facilities, supervised the research group, conceived the initial study concept,

**Table 5.** Proportion of total area and area within each recovery unit and tortoise conservation area that experienced an increase in OHV route density between 1980 and 2020.

Recovery unit	Tortoise conservation areas						
<b>Colorado Desert</b>	CM 7.47% (3377 km <sup>2</sup> )	AG 6.78% (379 km <sup>2</sup> )	CK 7.24% (79 km <sup>2</sup> )	FE 7.68% (375 km <sup>2</sup> )	JT 9.81% (269 km <sup>2</sup> )	PT 6.74% (230 km <sup>2</sup> )	PV 8.44% (90 km <sup>2</sup> )
<b>Northeastern Mojave Desert</b>				BD 10.78% (140 km <sup>2</sup> )	CS 8.09% (98 km <sup>2</sup> )	GB 8.46% (259 km <sup>2</sup> )	MM 12.73% (192 km <sup>2</sup> )
<b>Western Mojave Desert</b>					FK 9.88% (306 km <sup>2</sup> )	OR 8.30% (138 km <sup>2</sup> )	SC 8.18% (383 km <sup>2</sup> )
<b>Eastern Mojave Desert</b>						EV 9.22% (149 km <sup>2</sup> )	IV 6.93% (268 km <sup>2</sup> )
<b>Upper Virgin River</b>							RC 7.37% (26 km <sup>2</sup> )

The percentage values represent the proportion of the total area within each TCA that saw an increase in OHV route density, while the values in square kilometers (km<sup>2</sup>) indicate the actual area that experienced this increase. Tortoise conservation areas are abbreviated as follows: AG = Chocolate Mountain Aerial Gunnery Range; BD = Beaver Dam Slope; CK = Chuckwalla; CM = Chemehuevi; CS = Coyote Springs; EV = Eldorado Valley; FE = Fenner; FK = Fremont-Kramer; GB = Gold Butte-Pakoon; IV = Ivanpah; JT = Joshua Tree National Park; MM = Mormon Mesa; OR = Ord-Rodman; PT = Pinto Mountains; PV = Piute Valley; RC = Red Cliffs Reserve; SC = Superior-Cronease.

assisted in the study design, data analysis, interpretation of data, manuscript writing, and manuscript review.

## Conflict of Interest

We report no conflicts of interest.

## Data Availability Statement

The source code for our model development is available at <https://github.com/csp-inc/blm-pva-ohv>. Example annotated images from our training data sets and route density layers are available at <https://doi.org/10.6084/m9.figshare.28617044>.

## References

- Allison, L.J. & McLuckie, A.M. (2018) Population trends in Mojave desert tortoises (*Gopherus agassizii*). *Herpetological Conservation and Biology*, **13**, 433–452.
- Averill-Murray, R.C. & Allison, L.J. (2023) Travel management planning for wildlife with a case study on the Mojave desert tortoise. *Journal of Fish and Wildlife Management*, **14**, 269–281. Available from: <https://doi.org/10.3996/JFWM-22-030>
- Bates, D., Maechler, M., Bolker, B. & Walker, S. (2015) Fitting linear mixed-effects models using lme4. *Journal of Statistical Software*, **67**, 1–48. Available from: <https://doi.org/10.18637/jss.v067.i01>
- Boarman, W.I. & Sazaki, M. (2006) A highway's road-effect zone for desert tortoises (*Gopherus agassizii*). *Journal of Arid Environments*, **65**, 94–101. Available from: <https://doi.org/10.1016/j.jaridenv.2005.06.020>
- Brattstrom, B.H. & Bondello, M.C. (1983) Effects of off-road vehicle noise on desert vertebrates. In: Webb, R.H. & Wilshire, H.G. (Eds.) *Environmental effects of off-road vehicles: impacts and management in arid regions*. New York: Springer-Verlag, pp. 167–206.
- Brooks, M. & Lair, B. (2005) *Ecological effects of vehicular routes in a desert ecosystem*. Henderson, NV: United States Geological Survey, Western Ecological Research Center, Las Vegas Field Station.
- Buckley, R. (2004) Environmental impacts of off-highway vehicles. In: Buckley, R. (Ed.) *Environmental impacts of ecotourism*. Wallingford, UK: CABI Publishing, pp. 83–97.
- Cohen, J.B., Durkin, M.M. & Zdravkovic, M. (2014) Human disturbance of snowy plovers (*Charadrius nivosus*) in northwest Florida during the breeding season. *Florida Field Naturalist*, **42**, 1–14.
- Csurka, G., Volpi, R. & Chidlovskii, B. (2022) Semantic image segmentation: two decades of research. *Foundations and Trends in Computer Graphics and Vision*, **14**(162), 1.
- Custer, N.A., DeFalco, L.A., Nussear, K.E. & Esque, T.C. (2017) Drawing a line in the sand: effectiveness of off-highway vehicle management in California's Sonoran desert. *Journal of Environmental Management*, **193**, 448–457. Available from: <https://doi.org/10.1016/j.jenvman.2017.02.033>
- Deng, J., Dong, W., Socher, R., Li, L.-J., Li, K. & Fei-Fei, L. (2009) ImageNet: a large-scale hierarchical image database.

- In: *2009 IEEE conference on computer vision and pattern recognition*. Miami, FL: IEEE, pp. 248–255. Available from: <https://doi.org/10.1109/CVPR.2009.5206848>
- Dewitz, J. (2023) National Land Cover Database (NLCD) 2021 Products. <https://doi.org/10.5066/P9JZ7AO3>
- Esque, T.C., DeFalco, L.A., Tyree, G.L., Drake, K.K., Nussear, K.E. & Wilson, J.S. (2021) Priority species lists to restore desert tortoise and pollinator habitats in Mojave Desert shrublands. *Natural Areas Journal*, **41**, 145–158.
- Giorgiani do Nascimento, R. & Viana, F. (2020) Satellite image classification and segmentation with transfer learning. *AIAA Scitech 2020 Forum*, 1864. Available from: <https://doi.org/10.2514/6.2020-1864>
- Goodfellow, I., Bengio, Y. & Courville, A. (2016) *Deep learning (adaptive computation and machine learning series)*. Cambridge, UK: MIT Press.
- Gorelick, N., Hancher, M., Dixon, M., Ilyushchenko, S., Thau, D. & Moore, R. (2017) Google earth engine: planetary-scale geospatial analysis for everyone. *Remote Sensing of Environment*, **202**, 18–27.
- Gray, M.E., Dickson, B.G., Nussear, K.E., Esque, T.C. & Chang, T. (2019) A range-wide model of contemporary, omnidirectional connectivity for the threatened Mojave desert tortoise. *Ecosphere*, **10**, e02847. Available from: <https://doi.org/10.1002/ecs2.2847>
- He, K., Zhang, X., Ren, S. & Sun, J. (2016) Deep residual learning for image recognition. In: *Proceedings of the IEEE conference on computer vision and pattern recognition (CVPR)*, pp. 770–778. [https://openaccess.thecvf.com/content\\_cvpr\\_2016/html/He\\_Deep\\_Residual\\_Learning\\_CVPR\\_2016\\_paper.html](https://openaccess.thecvf.com/content_cvpr_2016/html/He_Deep_Residual_Learning_CVPR_2016_paper.html)
- He, Y., Franklin, S.E., Guo, X. & Stenhouse, G.B. (2009) Narrow-linear and small-area forest disturbance detection and mapping from high spatial resolution imagery. *Journal of Applied Remote Sensing*, **3**, 033570. Available from: <https://doi.org/10.1117/1.3283905>
- Hijmans, R.J., Bivand, R., Forner, K., Ooms, J., Pebesma, E. & Sumner, M.D. (2022) Package ‘terra’. Vienna Austria: Maint.
- Hoeser, T. & Kuenzer, C. (2020) Object detection and image segmentation with deep learning on earth observation data: a review-part I: evolution and recent trends. *Remote Sensing*, **12**, 1667. Available from: <https://doi.org/10.3390/rs12101667>
- Howard, J. & Gugger, S. (2020) Fastai: a layered API for deep learning. *Information*, **11**, 108. Available from: <https://doi.org/10.3390/info11020108>
- Jakes, A.F., Jones, P.F., Paige, L.C., Seidler, R.G. & Huijser, M.P. (2018) A fence runs through it: a call for greater attention to the influence of fences on wildlife and ecosystems. *Biological Conservation*, **227**, 310–318.
- Lamba, A., Cassey, P., Segaran, R.R. & Koh, L.P. (2019) Deep learning for environmental conservation. *Current Biology*, **29**, R977–R982. Available from: <https://doi.org/10.1016/j.cub.2019.08.016>
- Lechner, A.M., Stein, A., Jones, S.D. & Ferwerda, J.G. (2009) Remote sensing of small and linear features: quantifying the effects of patch size and length, grid position and detectability on land cover mapping. *Remote Sensing of Environment*, **113**, 2194–2204. Available from: <https://doi.org/10.1016/j.rse.2009.06.002>
- Lendemer, J., Thiers, B., Monfils, A.K., Zaspel, J., Ellwood, E.R., Bentley, A. et al. (2020) Corrigendum: the extended specimen network: a strategy to enhance US biodiversity collections, promote research and education. *Bioscience*, **70**, 195. Available from: <https://doi.org/10.1093/biosci/biz165>
- Lovich, J.E. & Bainbridge, D. (1999) Anthropogenic degradation of the southern California desert ecosystem and prospects for natural recovery and restoration. *Environmental Management*, **24**, 309–326. Available from: <https://doi.org/10.1007/s002679900235>
- Monz, C.A., Cole, D.N., Leung, Y.F. & Marion, J.L. (2010) Sustaining visitor use in protected areas: future opportunities in recreation ecology research based on the USA experience. *Environmental Management*, **45**, 551–562.
- Najjar, A., Kaneko, S. & Miyanaga, Y. (2017) Combining satellite imagery and open data to map road safety. *Proceedings of the AAAI Conference on Artificial Intelligence*, **31**(1). Available from: <https://doi.org/10.1609/aaai.v31i1.11168>
- Nussear, K.E., Esque, T.C., Inman, R.D., Gass, L., Thomas, K.A. & Wallace, C.S.a. (2009) Modeling habitat of the desert tortoise (*Gopherus agassizii*) in the Mojave and parts of the Sonoran Deserts of California, Nevada, Utah, and Arizona.
- Paszke, A. (2019) Pytorch: An imperative style, high-performance deep learning library. arXiv preprint arXiv:1912.01703.
- R Core Team. (2018) R: A Language and Environment for Statistical Computing. Available from: <https://www.r-project.org/>
- Richardson, M.L., Wilson, B.A., Aiuto, D.A., Crosby, J.E., Alonso, A., Dallmeier, F. et al. (2017) A review of the impact of pipelines and power lines on biodiversity and strategies for mitigation. *Biodiversity and Conservation*, **26**, 1801–1815.
- Ripley, B.D. & Venables, W.N. (2002) *Modern applied statistics with S*, fourth. New York: Springer. Available from: <https://www.stats.ox.ac.uk/pub/MASS4/>
- Robillard, A., Trizna, M., Ruiz-Tafur, M., Dávila Panduro, E.L., de David Santana, C., White, A. et al. (2023) Application of a deep learning image classifier for identification of Amazonian fishes. *Ecology and Evolution*, **13**, e9987. Available from: <https://doi.org/10.1002/ece3.9987>
- Sizek, J. (2024) Impossible evidence: the legal dismal cycle of regulating off-roading in the California desert. *Geoforum*, **149**, 103941. Available from: <https://doi.org/10.1016/j.geoforum.2024.103941>
- Smith, W. (2021) Remote detection of disturbance from motorized vehicle use in Appalachian wetlands. *Virginia Journal of Science*, **72**(3), 1.

- Sohl, T., Reker, R., Bouchard, M., Sayler, K., Dornbierer, J., Wika, S. et al. (2016) Modeled historical land use and land cover for the conterminous United States. *Journal of Land Use Science*, **11**, 476–499. Available from: <https://doi.org/10.1080/1747423X.2016.1147619>
- Switalski, T.A. & Jones, A. (2012) Off-road vehicle best management practices for forestlands: a review of scientific literature and guidance for managers. *Journal of Conservation Planning*, **8**, 12–24.
- U.S. Census Bureau. (2022) US Census Bureau TIGER/Line shapefiles. Available from: <https://www.census.gov/cgi-bin/geo/shapefiles/index.php>
- U.S. Department of Agriculture. (2022) *National Agriculture Imagery Program (NAIP)*. USDA NAIP GeoHub. Available from: <https://naip-usdaonline.hub.arcgis.com/> [Accessed 1st June 2022]
- U.S. Department of the Interior, Bureau of Land Management. (2019) Western Mojave (WEMO) route network project final supplemental environmental impact statement for the California desert district.
- U.S. Fish and Wildlife Service. (2011) Revised recovery plan for the Mojave population of the desert tortoise (*Gopherus agassizii*). Available from: <https://www.fws.gov/sites/default/files/documents/USFWS.2011.RRP%20for%20the%20Mojave%20Desert%20Tortoise.pdf>
- U.S. Geological Survey. (2007) Environmental effects of off-highway vehicles on Bureau of Land Management lands: A literature synthesis. Available from: <https://pubs.usgs.gov/of/2007/1353/report.pdf> <https://doi.org/10.3133/ofr20071353>
- U.S. Geological Survey. (2018) *USGS EROS archive - aerial photography - digital Orthophoto quadrangle (DOQs)*. Sioux Falls, South Dakota, USA: Earth Resources Observation and Science (EROS) Center. Available from: <https://www.usgs.gov/centers/eros/science/usgs-eros-archive-aerial-photography-national-agriculture-imagery-program-naip#science>
- Van Etten, A. (2018) You only look twice: rapid multi-scale object detection in satellite imagery. Available from: <http://arxiv.org/abs/1805.09512> [Accessed 21st February 2024]
- Vincent, O.R. & Folorunso, O. (2009) A descriptive algorithm for sobel image edge detection. In: *Proceedings of informing science and IT education conference (InSITE)*, pp. 97–107. <https://proceedings.informingscience.org/InSITE2009/>
- InSITE09p097-107Vincent613.pdf [Accessed 1st February 2024]
- Weinstein, B.G. (2018) A computer vision for animal ecology. *The Journal of Animal Ecology*, **87**, 533–545. Available from: <https://doi.org/10.1111/1365-2656.12780>
- Weinstein, B.G., Marconi, S., Bohlman, S.A., Zare, A. & White, E.P. (2020) Cross-site learning in deep learning RGB tree crown detection. *Ecological Informatics*, **56**, 101061. Available from: <https://doi.org/10.1016/j.ecoinf.2020.101061>
- Westcott, F. & Andrew, M.E. (2015) Spatial and environmental patterns of off-road vehicle recreation in a semi-arid woodland. *Applied Geography*, **62**, 97–106. Available from: <https://doi.org/10.1016/j.apgeog.2015.04.011>
- Xie, Y., Bhojwani, R., Shekhar, S. & Knight, J. (2018) An unsupervised augmentation framework for deep learning based geospatial object detection: a summary of results. In: *Proceedings of the 26th ACM SIGSPATIAL international conference on advances in geographic information systems*. New York, NY, USA: Association for Computing Machinery, pp. 349–358. Available from: <https://doi.org/10.1145/3274895.3274901>
- Yang, R., Ahmed, Z.U., Schulthess, U.C., Kamal, M. & Rai, R. (2020) Detecting functional field units from satellite images in smallholder farming systems using a deep learning based computer vision approach: a case study from Bangladesh. *Remote Sensing Applications: Society and Environment*, **20**, 100413. Available from: <https://doi.org/10.1016/j.rsase.2020.100413>

## Supporting Information

Additional supporting information may be found online in the Supporting Information section at the end of the article.

**Data S1.** Supporting Information.

**Appendix S0.** Sobel filter and image preprocessing.

**Appendix S1.** Data annotation.

**Appendix S2.** Image postprocessing.

**Appendix S3.** Trend visualization.

**Appendix S4.** Trend modeling.

**Appendix S5.** Trend analysis results.

**Appendix S6.** TCAs and RUs discussion.